Image reconstruction method for laminar optical tomography with only a single Monte-Carlo simulation

Mengyu Jia (贾梦宇)[1], Shanshan Cui (崔姗姗)[1], Xueying Chen (陈雪影)[1], Ming Liu (刘 明)[1], Xiaoqing Zhou (周晓青)[1], Huijuan Zhao (赵会娟)[1,2*], and Feng Gao (高 峰)[1,2]

[1] *College of Precision Instrument and Optoelectronics Engineering, TianjinUniversity, Tianjin 300072, China*

[2] *Tianjin Key Laboratory of Biomedical Detecting Techniques and Instruments, Tianjin 300072, China*

[*] *Corresponding author: huijuanzhao@tju.edu.cn*

Received October 29, 2013; accepted January 15, 2014; posted online February 28, 2014

Laminar optical tomography (LOT) is a new mesoscopic functional optical imaging technique. Currently, the forward problem of LOT image reconstruction is generally solved on the basis of Monte-Carlo (MC) methods. However, considering the nonlinear nature of the image reconstruction in LOT with the increasing number of source positions, methods based on MC take too much computation time. This letter develops a fast image reconstruction algorithm based on perturbation MC (pMC) for reconstructing the absorption or scattering image of a slab medium, which is suitable for LOT or other functional optical tomography system with narrow source-detector separation and dense sampling. To calculate the pMC parameters, i.e., the path length passed by a photon and the collision numbers experienced in each voxel with only one baseline MC simulation, we propose a scheme named as the trajectory translation and target voxel regression (TT&TVR) based on the reciprocity principle. To further speed up the image reconstruction procedure, the weighted average of the pMC parameters for all survival photons is adopted and the region of interest (ROI) is extracted from the raw data to save as the prior information of the image reconstruction. The method is applied to the absorption reconstruction of the layered inhomogeneous media. Results demonstrate that the reconstructing time is less than 20 s with the $X-Y$ section of the sample subdivided into 50×50 voxels, and the target size quantitativeness ratio can be obtained in a satisfying accuracy in the source-detector separations of 0.4 and 1.25 mm, respectively.

OCIS codes: 170.3880, 170.6960, 170.5280, 170.3660, 170.3010.

doi: 10.3788/COL201412.031702.

Laminar optical tomography (LOT) uses a system similar to a confocal microscope[1−3], which adopts galvanometer mirrors to scan a focused laser beam over the sample, and detects the slightly diffused light both from the focus of the scanning beam and at the increasing distances (from 0 to 3 mm away) from the source. Then, the light irradiates the next source position, and the detection is repeated. At last, the images of the distribution of absorption coefficient ($\mu_{\rm a}$) or the reduced scattering coefficient ($\mu_{\rm s}'$) are reconstructed in the similar way to the diffuse optical tomography (DOT). It thus can be seen that the high resolution images can be acquired provided that enough sample points are available[3], for example more than 2500 source positions per square centimeter are needed for obtaining a spatial resolution of 200 μm. Researchers have proved that as the source-detector separation is narrower than 1 mm, the standard diffusion approximation (DA) based approaches, e.g., the diffusion equation (DE) and the more complicated three-order (P3) approximation equation, leads to large errors in modeling light propagation in tissue[4,5]. Since the Monte-Carlo (MC) method owns prominent advantages in solving the radiative transfer equation more accurately than DA, and easily being adapted to tissue with arbitrary geometries[6,7], it is one of promising methods for solving the forward problem of image reconstruction in LOT.

To obtain a convergent solution, MC simulation costs a lot of time normally, thus the idea for estimating derivatives from a single or several MC simulation (s) is proposed. Tuchin[8] developed condensed MC (CMC) using a scaling procedure to increase the efficiency of the MC. Similarly, Liu *et al.*[7] presented another scaling method. Pfefer *et al.*[9] employed a neural-network algorithm trained on phantoms to extract optical parameters from target phantoms. Zhao *et al.*[10] presented a fast inverse MC (IMC) scheme based on look-up table for extracting both $\mu_{\rm a}$ and $\mu_{\rm s}$, but it was only adopted for imaging a single point of the object. However, all the above schemes are only suitable for homogeneous media and thus cannot be applied to image reconstruction of inhomogeneous media. Perturbation MC (pMC) method presented by Hayakawa *et al.*[11] can calculate both $\mu_{\rm a}$ and $\mu_{\rm s}$ simultaneously for inhomogeneous media, however, it is required to run many baseline MC simulations for different source positions and thus has not been yet applied to LOT system.

In the investigation of image reconstruction algorithm for LOT, Boas *et al.*[1] proposed a method by combing Beer's law with MC simulation to establish a lookup table and calculate the $\mu_{\rm a}$ of target. However, the method is based on the assumption that the physical size and position of the target is known. Dunn *et al.*[12] developed a reconstruction algorithm based on the first Born approximation to the radiative transport equation to reconstruct an absorption image. By calculating sensitivity functions from MC, Hillman *et al.*[3] use Tikhonov regularization to map the LOT raw measurements into

 © 2014 Chinese Optics Letters

a three-dimensional (3D) image of absorption changes. To avoid running MC simulations in each iteration step during image reconstruction, these two methods relies on the linearization assumptions, and thus are applicable to the target with small absorption disturbance and no scattering coefficient contrast to the background. In general, the μ_a value at which the linear approximation breaks down varies depending on the size and depth the perturbation[12].

This letter aims at developing a fast forward calculation scheme based on the pMC for the nonlinear image reconstruction of LOT. The method can achieve the pMC parameters (i.e., the path length and the collision numbers) from a single MC simulation for all the source positions.

Considering a LOT system for early detection of carcinoma *in situ* (CIS), such as cervical and cutaneous cancer, a sample with the similar optical parameters to those of cervical epithelium is adopted in this letter. As illustrated in Fig. 1(a), to obtain a high spatial resolution, 50×50 scanning spots (the black dots) are assumed on the $X-Y$ plane and the sample is uniformly divided into 50×50 voxels (for simplicity, only 8×8 voxels are shown in Fig. 1(a)) with the scanning spots locating on the end points of the voxels on the $X-Y$ plane. The source and detector positions are raster scanned to cover the whole detection region.

To avoid running many baseline MC simulations for different source positions while adopting pMC method, we develop a scheme named as the trajectory translator and target voxel regression (TT&TVR) to achieve the pMC parameters from a single MC simulation in the homogeneous media. As shown in Fig. 1(a), suppose that the detection region is in the 1st quadrant, $S-D$ and $S'-D'$ are the two source-detector pairs at different measuring times with the fixed separation, and S is the first scanning position locating at the origin of the coordinate. For a source position $S' \neq S$, the target voxel (labeled in E_n) may locate at four orientations to the source. According to the reciprocity principle, light propagation between a source-detector pair and a voxel remains the same after mirror translation is conducted to them[13]. Then, considering a homogenous medium, we can find some equivalent relations, e.g., the calculated MC results for voxel E_1 from the irradiation on S' and detection from D' are the same as those for E'_1 but with irradiation on S and detection from D.

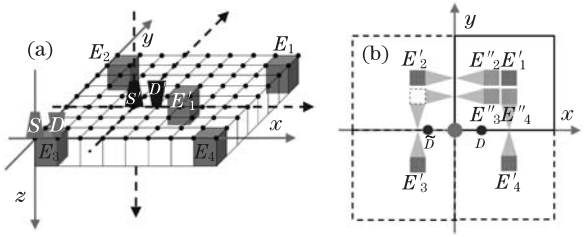

Fig. 1. (a) Schematic map of the source-detector distribution and the principle of trajectory translation. E_n represents voxel, $S(S')$ and $D(D')$ represents source and detector positions respectively. (b) Principle of the target voxel regression. The region within the black solid line represents the real detection region showed in (a), $\widetilde{D}$ and D locates at both sides of the source symmetrically.

On the basis of the above considerations, to obtain the pMC parameters of all the scanning spots from a single running of MC with the source-detector position located on $S-D$, the forward steps can be adopted.

Step 1 is to obtain the pMC parameters for the source position S locating at (0, 0) and the detection positions D and $\widetilde{D}$.

A mirror site $\widetilde{D}$ is adopted, i.e., D and $\tilde{D}$ locates at both sides of the source symmetrically, as shown in Fig. 1(b). Since only one source position is involved, one single MC simulation is enough to get the required pMC parameters for all the voxels. The pMC parameters include the path length $l_{i,k}(D_j)$ and collision numbers $c_{i,k}(D_j)$ with subscript representing the kth photon detected by the jth detector D_j and visiting the ith voxel.

Step 2 is to obtain the pMC parameters by TT&TVR when the scanning in LOT is performed, i.e., source-detector pair moves to the other positions within the detection area.

Since the separation and orientation between the source and detection points keeps unchanged, to use the results in Step 1, we introduce the method of TT, i.e., the other source-detector pairs are translated to $S-D$ and the target voxels are also "moved" to the corresponding positions, respectively. For example, for the target voxels E_1, E_2, E_3, and E_4 in Fig. 1(a), after the translation of $S'-D'$ to $S-D$ the target voxels will be "moved"to E'_1, E'_2, E'_3, and E'_4, respectively, as shown in Fig. 1(b) by keeping the number of voxels along the photon transportation track unchanged. As we can see from Fig. 1(b), the E'_1, E'_2, E'_3, and E'_4 may locate not only in the 1st quadrant but also in the other three quadrants. To use the results obtained in Step 1 that only deals with the voxels in the 1st quadrant, based on the reciprocity principle, TVR is developed to find the virtual target voxels locating in the 1st quadrant but being equivalent to E'_2, E'_3, and E'_4, respectively, from the view of obtaining pMC parameters. In the following, we will demonstrate that the virtual target voxel does exist and can be obtained.

1) For the voxel E'_4 locating on the 4th quadrant, the virtual voxel E''_4 can be simply obtained from mirror transformation about X axis under the consideration that the light propagation between $S-E''_4-D$ is effectively equivalent to $S-E'_4-D$;

2) For the voxel E'_2 locating on the 2nd quadrant, the virtual voxel E''_2 is also determined from mirror transformation about Y axis;

3) For the voxel E'_3 locating on the 3rd quadrant, the virtual voxel E''_3 is obtained through the mirror transformation about Y axis firstly and subsequently about X axis or vice versa.

Step 3: Considering a medium with inhomogeneity, based on the above results for homogenous medium, photon weight obtained at the source S and detector$D$ can be reweighted[11,14].

$$w'_{S,D} = w_{S,D} \prod_m \xi(D_1) \prod_n \xi(D_2), \tag{1}$$

where $w_{S,D}$ is the photon weight for a homogenous medium with the same optical properties as those of the background of the inhomogeneous medium; $\xi(D_j) = \left[\frac{\mu_{s,I}(r_i)}{\mu_{s,B}(r_i)}\right]^{\overline{c_i(D_j)}} \exp\left\{[\mu_{t,B}(r_i) - \mu_{t,I}(r_i)]\,\overline{l_i(D_j)}\right\}$

with $\mu_{\rm t} = \mu_{\rm a} + \mu_{\rm s}$ being the total attenuation coefficient; $\mu_{\rm s}(r_i)$ and $\mu_{\rm t}(r_i)$ being the scattering and total attenuation coefficient of the ith voxel, respectively; the subscript I and B indicating the inhomogeneity and background; m is the total number of voxels in the dynamically defined 1st and 4th quadrants by assigning the current scanning spot as the origin of the coordinate, and n is that in the dynamically defined 2nd and 3rd quadrants.

With the scheme described above, it can be found that only a single run of MC calculation as listed in Step 1 is needed for obtaining the pMC parameters for the LOT measurement in an inhomogeneous medium.

In the traditional pMC method, the trajectory database of all the received photons in a baseline MC simulation must be recorded, which not only requires a huge memory space of computer (e.g., a total memory of 10 Gb is needed for 2.4×10^5 survival photons[14]), but also leads the saving time to be the major portion in the baseline MC simulation. In this letter, we take the weighted average of $l_{i,k}(D_j)$ and $c_{i,k}(D_j)$, the weighting coefficients are equal to the weight of the kth launched photon respectively. As a result, the requirement of the memory space as well as the reconstruction time are both diminished.

The whole flow of the inverse calculation is similar to that of DOT[15]. To begin with, the Jacobi matrix $J_{S,D}$ is got by a closed-form differentiation or numerical differentiation of Eq. (1). Since the common regularization methods based on the 2-norm, e.g., conjugate gradient, algebraic reconstruction techniques (ART), and Tikhonov, are continues or piecewise continuous, the reconstructed images are unavoidably blurry in edges. Considering the high spatial resolution of LOT, and the sparse detected signal[1], the *l1_ls* method[16] based on 1-norm is adopted.

In general, raw image of PMT itself acquired with the LOT system possesses high spatial resolution in case of dense scanning[3], which means that we can determine the region of interest (ROI) from the raw image of PMT by image segmentation based on the level set method. If only the measurement data within ROI were adopted and subsequently only the optical parameters of ROI were reconstructed, the dimension of $J_{S,D}$ and $\overrightarrow{b}$ can be further lessened and the reconstruction procedure will be considerably accelerate.

The performance of the proposed method is evaluated using the simulation data for a slab sample, as shown in Fig. 2.

Suppose that 50×50 scanning spots are distributed uniformly in an area of 20×20 (mm). In the forward calculation the sample is subdivided into 50×50 voxels along the Z direction uniformly, i.e., the side length of the voxel is equal to the interval between the adjacent scanning spots. The voxel has a hight of 0.7 mm, referring to the general thickness of CIS. The background optical parameters are assumed as $\mu_{\rm a0}$= 0.1 mm^{-1}, μ_{s0}=4 mm^{-1}, anisotropic coefficient g=0.9, and refractive index n=1.4 for describing the optical properties of cervical epithelial in 632.8 nm[13]. Since the information of oxy-and deoxy-hemoglobin concentration only relates to the absorption coefficient, in the following, the scattering coefficient of the heterogeneity is set to be the same as that of the background.

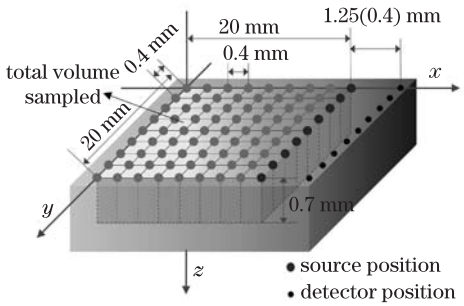

Fig. 2. Sample and the distribution of the scanning spot for generating simulation data.

Concerning the source-detector separation adopted in LOT system for the early detection of CIS, we select 0.4 and 1.25 mm as the narrow and wide source-detector separation to evaluate the proposed method respectively. For the source-detector separation of 0.4 mm, the "measurement" data are calculated from the forward model as described above and noise is added in the "measurement" data as an additive Gaussian random variable with a standard deviation $\sigma(t_p)$ proportional to the transient intensity[17], i.e., $\sigma(t_p) = \Gamma(t_p)\,10^{-\eta/20}$, where $\Gamma(t_p)$ is the the pth normally distributed pseudorandom number and η is the signal-to-noise ratio (SNR) in decibels. For the source-detectors eparation of larger than 1 mm, the "measurement" data are generated from DE solved by finite element method (FEM) to avoid the inverse crime. From the investigation, we find that the advisable value of *l1_ls* regularization parameter is $0.0042 * ||2J_{S,D}^T \overrightarrow{b}||_\infty$ with $\overrightarrow{b}$ the matrix of the "measurement" data.

ROI is determined based on the level set method, the coefficient of the weighted length term, coefficient of the internal energy term, coefficient of the weighted area term, and time step are set to 3.5, 0.2, 2.5, and 5.0 successively. All the reconstructions were performed on a PC with 2.8 GHz Intel Core i5-2300CPU and 4-Gb RAM. The results are evaluated in terms of the quantitativeness ratio (QR), full width half maximum (FWHM), and spatial resolution. QR is defined as the ratio of the optical property difference between the reconstructed target and the background to the real difference.

A heterogeneous target is laid at the center of the sample with a size of $2 \times 2 \times 0.7$ (mm) to mimic the cancerous area. When the source-detector separation is set as 1.25 mm, the images for the target absorption contrast (TAC) from 1.5 to 5 at an increment of 0.5 are reconstructed. Table 1 presents the QR and FWHM of the target in the reconstructed images, and, as examples, Fig. 3 shows the reconstructed $\mu_{\rm a}$ images with TAC of 2, 3.5, and 5, respectively. It is observed from Table 1 that more than 93% of QR is achieved for all the TAC cases, and little difference exists in there constructed target size according to the FWHM data. However, if the linear image reconstruction algorithm are adopted, the achieved QR is only 59.51% (results are not shown), which further indicate the effectiveness of our proposed method.

For the above one target sample, but with source-detector separation of 0.4 mm, the reconstruction perfor-

Table 1. Reconstruction Performance for One Target Sample with Source-Detector Separation of 1.25 mm

TAC	1.5	2.0	2.5	3.0	3.5	4.0	4.5	5.0
QR (%)	94.8	94.7	94.5	94.4	94.2	94.0	93.9	93.7
FWHM (mm)	2.05	2.05	2.05	2.05	2.05	2.04	2.04	2.04

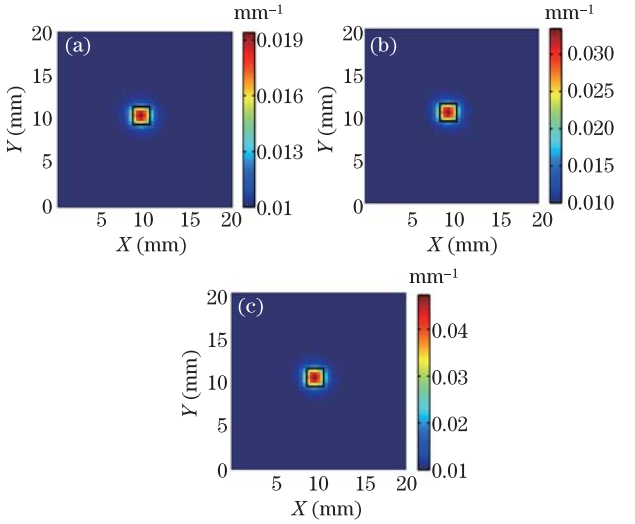

Fig. 3. (Color online) Reconstructed μ_a images of the one target sample with the source-detector separation of 1.25 mm, and the absorption coefficient being (a) 0.02, (b) 0.035, and (c) 0.05 mm^{-1}. The black solid lines indicate the original target.

Table 2. Reconstruction Performance for One Target Sample with Source-Detector Separation of 0.4 mm

TAC	1.5	2.0	2.5	3.0	3.5	4.0	4.5	5.0
QR (%)	99.5	97.3	95.7	96.1	95.7	95.4	94.0	94.5
FWHM (mm)	2.0	2.0	2.0	2.0	2.0	2.0	2.0	2.0

mance is listed in Table 2 and some of the images are shown in Fig. 4. The minimum SNR tolerated by the algorithm lies around 25 dB, here we add a noise to obtain η= 30 dB. Comparing to Fig. 3, we can see that the target size and location are in more agreement with the actual situation.

The possible reasons responsible for the lower accuracy in target size and location in Fig. 3 than those in Fig. 4 are the improper subdivision grid in FEM, unsuitable model with DE[1], and also the lower spatial resolution caused by the wider source-detector separation.

To evaluate the spatial resolution of the reconstructed images, a sample with two targets is employed. A fixed target absorption contrast of 2 is assumed.

Figure 5(a) illustrates the reconstructed μ_a images for the sample at the edge-to-edge separation (EES) of 1.4, 1.0, and 0.6 mm, respectively, while the source-detector separation is 1.25 mm. To quantify the spatial resolution performance of thereconstructed images, we introduce a measure defined as $R = [M_{a_{max}} - \mu'_a]/(M_{a_{max}} - M_{a_{min}})$, with $M_{a_{max}}$, $M_{a_{min}}$, and μ'_a being the maximum, the minimum, and the value at x = 9.5 mm of the profilealong the X-axis at y=9.5 mm of the reconstructed image, respectively. According to the characteristics of the human vision system, it is normally assumed that two targets are distinguishable for $R > 0.1$. As shown in Fig. 5(b), in the EESs listed above, R is 0.79, 0.6, and 0.35, respectively.

For a source-detector separation of 0.4 mm, concerning that the spatial resolution of LOT image is improved with the reduction of source-detector separation, the EES of 1.2, 0.8, and 0.4 mm, respectively, is adopted. Figure 6(a) shows the reconstructed absorption images of the sample with two targets. It is seen that the locations of the two targets are reconstructed correctly. Regarding the spatial resolution, R is 0.9, 0.72, and 0.4 respectively, as can be seen in Fig. 6(b).

For all the test cases above, the proposed reconstruction algorithm converges in less than 11 iterations (∼20 s), which is only about 1/10 of that needs by the traditional pMC method.

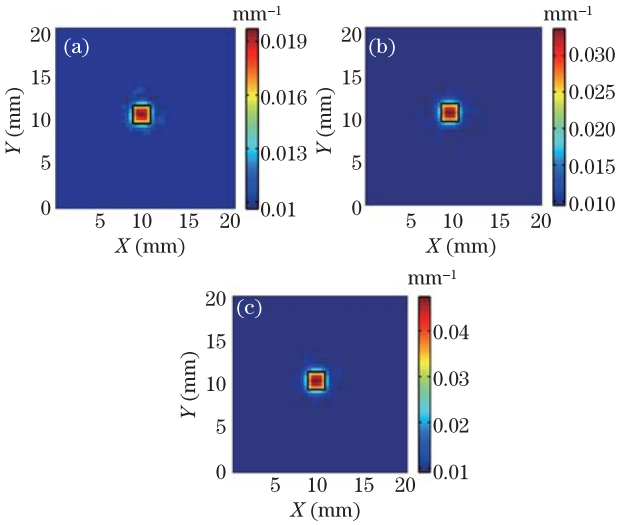

Fig. 4. (Color online) Reconstructed μ_a images of the one target sample with the source-detector separation being 0.4 mm, and the absorption coefficient being (a) 0.02, (b) 0.035, and (c) 0.05 mm^{-1}. The black solid lines indicate the original target.

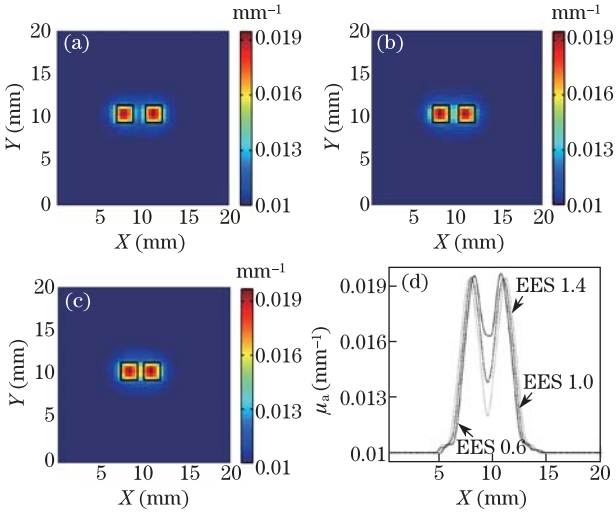

Fig. 5. (Color online) Reconstructed μ_a images of the sample with two target sin the source-detector separation of 1.25 mm for EES =(a) 1.4, (b) 1.0, and (c) 0.6 mm, respectively. The black solid lines indicate the original targets. (d) The profile along the X-axis at y=9.5 mm.

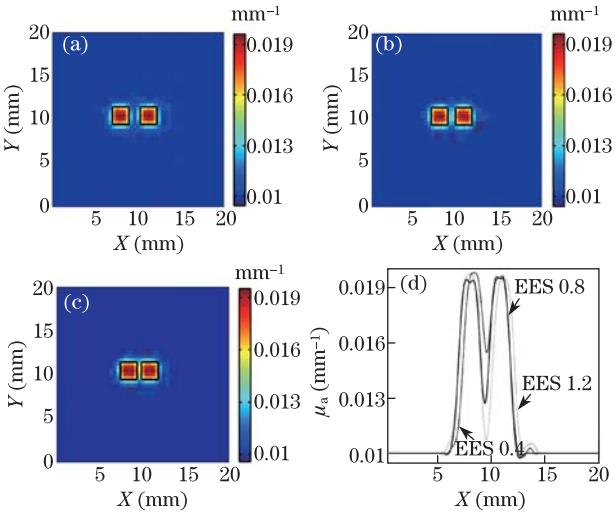

Fig. 6. (Color online) Reconstructed μ_a images of sample with two targets in the source-detector separation of 0.4 mm for EES=(a) 1.2, (b) 0.8, and (c) 0.4 mm, respectively. The black solid lines indicate the original targets. (d) The profile along the X-axis at y=9.5 mm.

The results indicate that both the method for forward problem calculation and that for the inverse problem calculation developed in this letter are capable of reconstructing images with reasonable accuracy for LOT.

In conclusion, this letter develops a fast scheme of the forward calculation based on the pMC for the image reconstruction with nonlinear procedure. The method is suitable for LOT or other functional optical tomography system with short source-detector separations and dense sampling. In essence, this proposed method involves three key steps: firstly, considering the multiple source positions in LOT, to introduce pMC method into the solution of the forward problem while avoid running multiple baseline MC simulations, we propose TT&TVR strategy based on reciprocity principle; secondly, in order to save computer memory for the baseline MC simulation and enhance the efficiency of reconstruction, the weighted average of the pMC parameters for all the detected photons is adopted; thirdly, taking advantage of the raw image in LOT, ROI is involved in the inverse problem as prior information to further accelerate the reconstructing process. Simulations of LOT measurement are conducted with source-detector separations of 0.4 and 1.25 mm, respectively. Results demonstrate that the proposed method shows great performance in terms of the QR, FWHM, and spatial resolution.

With the proposed method, the speeding of the reconstruction is achieved with the following two aspects: firstly, by adopting the weighted average, the pMC parameters needed to be processing in reconstruction is decreased by N times with N the total number of the survival photons; secondly, with the ROI being involved in the calculation of inverse problem, the scale of $J_{S,D}$ and $\vec{b}$ can be cut down dramatically, e.g., $J_{S,D}$ and $\vec{b}$ is only 1/670 and 1/26 of the original size, respectively.

Multiple measurements with different source-detector separations can be used for depth resolution and creating a 3D image of tissue[1−3]. Although the proposed method in this letter is only evaluated in the case of one source-detector separation, one can extend the proposed algorithm to treat measurements with multiple source-detector separations by simply creating the subdivision along the vertical direction.

Tis work was supported by the National Natural Science Foundation of China (Nos. 81271618, 81101106, and 61108081) and the Tianjin Municipal Government of China (Nos. 13JCZDJC28000 and 12JCQNJC09400).

References

1. D. A. Boas, C. Pitris, and N. Ramanujam, *Handbook of Biomedical Optics* (CRC Press, Boca Raton, 2011) pp. 359-373.
2. T. J. Muldoon, S. A. Burgess, B. R. Chen, D. Ratner, and E. M. Hillman, Biomed. Opt. Express **3,** 1701 (2012).
3. E. M. Hillman, and S. A. Burgess, Laser Photon. Rev. **3,** 159 (2009).
4. L. V. Wang and H. I. Wu, *Biomedical Optics: Principles and Imaging* (Wiley, New York, 2007).
5. D. Wang, J. Zhang, Y. Zhao, S. Chen, L. Yuan, J. Lei, C. Zhang, and S. Hou, Chin. Opt. Lett. **10,** 122301 (2012).
6. W. Cai and L. Ma, Chin. Opt. Lett. **10,** 012901 (2012).
7. Q. Liu and N. Ramanujam, J. Opt. Soc. Am. A **24,** 1011 (2007).
8. V. V. Tuchin, *Tissue Optics*: *Light Scattering Methods and Instruments for Medical Diagnosis* (SPIE Press, Bellingham, 2007).
9. T. J. Pfefer, L. S. Matchette, C. L. Bennett, J. A.Gall, J. N. Wilke, A. J. Durkin, and M. N. Ediger, J. Biomed. Opt. **8,** 206 (2003).
10. H. Zhao, X. Zhou, J. Liang, and S. Zhang, Chin. Opt. Lett. **6,** 935 (2008).
11. C. K. Hayakawa, J. Spanier, F. Bevilacqua, A. K. Dunn, J. S. You, B. J. Tromberg, and V. Venugopalan, Opt. Lett. **26,** 1335 (2001).
12. A. Dunn and D.Boas, Opt. Lett. **25,** 1777 (2000).
13. H. Liu, D. A. Boas, Y. Zhang, A. G. Yodh, and B. Chance, Phys. Med. Biol. **40,** 1983 (1995).
14. C. Zhu and Q. Liu, J. Biomed. Opt. **17,** 0105011 (2012).
15. X. Zhou, Y. Fan, Q. Hou, H. Zhao, and F. Gao, Appl. Opt. **52,** 1779 (2012).
16. Z. Lingling, W. Huaxiang, X. Yanbin, and W. Da, WSEAS Transactions on Circuits and Systems **10,** 393 (2011).
17. F. Yang, F. Gao, P. Ruan, and H. Zhao, Appl. Opt. **49,** 3111 (2010).